JOURNAL OF BACTERIOLOGY, Aug. 2008, p. 5368–5381 Vol. 190, No. 15
0021-9193/08/$08.00+0 doi:10.1128/JB.00044-08

Modes of Overinitiation, *dnaA* Gene Expression, and Inhibition of Cell Division in a Novel Cold-Sensitive *hda* Mutant of *Escherichia coli*▽

Kazuyuki Fujimitsu,† Masayuki Su'etsugu,†‡ Yoko Yamaguchi,†§ Kensaku Mazda,¶ Nisi Fu, Hironori Kawakami,‖ and Tsutomu Katayama*

Department of Molecular Biology, Graduate School of Pharmaceutical Sciences, Kyushu University, 3-1-1 Maidashi, Higashi-ku, Fukuoka 812-8582, Japan

Received 10 January 2008/Accepted 16 May 2008

The chromosomal replication cycle is strictly coordinated with cell cycle progression in *Escherichia coli*. ATP-DnaA initiates replication, leading to loading of the DNA polymerase III holoenzyme. The DNA-loaded form of the β clamp subunit of the polymerase binds the Hda protein, which promotes ATP-DnaA hydrolysis, yielding inactive ADP-DnaA. This regulation is required to repress overinitiation. In this study, we have isolated a novel cold-sensitive *hda* mutant, the *hda-185* mutant. The *hda-185* mutant caused overinitiation of chromosomal replication at 25°C, which most likely led to blockage of replication fork progress. Consistently, the inhibition of colony formation at 25°C was suppressed by disruption of the *diaA* gene, an initiation stimulator. Disruption of the *seqA* gene, an initiation inhibitor, showed synthetic lethality with *hda-185* even at 42°C. The cellular ATP-DnaA level was increased in an *hda-185*-dependent manner. The cellular concentrations of DnaA protein and *dnaA* mRNA were comparable at 25°C to those in a wild-type *hda* strain. We also found that multiple copies of the ribonucleotide reductase genes (*nrdAB* or *nrdEF*) or *dnaB* gene repressed overinitiation. The cellular levels of dATP and dCTP were elevated in cells bearing multiple copies of *nrdAB*. The catalytic site within NrdA was required for multicopy suppression, suggesting the importance of an active form of NrdA or elevated levels of deoxyribonucleotides in inhibition of overinitiation in the *hda-185* cells. Cell division in the *hda-185* mutant was inhibited at 25°C in a LexA regulon-independent manner, suggesting that overinitiation in the *hda-185* mutant induced a unique division inhibition pathway.

The initiation of chromosomal replication is strictly coordinated with cell cycle progression in prokaryotes and eukaryotes. In *Escherichia coli*, ATP-bound DnaA forms a specific complex with the chromosomal replication origin, *oriC* (22, 41), leading to the unwinding of duplex DNA in the AT-rich region of *oriC*. This process is stimulated by DiaA, a DnaA-binding protein that directly promotes the formation of the specific complex consisting of ATP-DnaA and *oriC* (21, 33). DnaB helicase is loaded onto the exposed single-stranded region of DNA by the DnaC helicase loader. In this process, DnaA promotes the reaction by directly binding to DnaB (1, 40, 54). The loaded DnaB helicase expands the single-stranded region, where DnaG primase and DNA polymerase III holoenzyme are sequentially loaded, leading to DNA replication (49). The cellular level of ATP-DnaA fluctuates with a peak at the time of the initiation of replication (36).

To repress extra initiation events, at least three pathways are found to function in vivo. The first is the inactivation of *oriC* by SeqA (38, 56). The minimal *oriC* region contains 11 repeats of the GATC sequence. Adenine residues in both of the strands within the palindromic GATC sequence are methylated by Dam (DNA adenine methyltransferase). Immediately after the synthesis of a nascent complementary strand, hemimethylated forms are transiently generated, and SeqA preferentially binds to these sites. The binding of SeqA to *oriC* prevents the formation of an active initiation complex on *oriC* (46), thus repressing extra initiations. Also, the *dnaA* promoter region contains the GATC sequence, and the postinitiation stage-specific repression of *dnaA* transcription depends on SeqA and Dam (6). The second pathway that functions to repress extra initiation events is the titration of DnaA molecules by the *datA* locus (34). The chromosomal locus *datA* contains five DnaA boxes which are 9-mer DnaA-binding sequences. This locus can bind to a considerable number of DnaA molecules, which therefore reduces the number of DnaA molecules that are accessible to *oriC*. The third system is the functional regulation of DnaA termed RIDA (for *r*egulatory *i*nactivation of *D*na*A*) (27). RIDA stimulates the hydrolysis of DnaA-bound ATP, yielding the inactive ADP-DnaA. This ATP hydrolysis depends on the DNA-loaded β sliding clamp and Hda (27, 29). The β sliding clamp is a subunit of the DNA polymerase III holoenzyme which is loaded on DNA during the process of DNA replication (49). Thus, cellular ATP-DnaA is converted to ADP-DnaA in a manner that is coordinated with replication and represses untimely extra initiation events.

Hda binds to the β sliding clamp via its short N-terminal region that contains the QL(S/D)LF motif that is conserved among clamp-binding proteins (10, 59). The binding of Hda to

* Corresponding author. Mailing address: Department of Molecular Biology, Graduate School of Pharmaceutical Sciences, Kyushu University, 3-1-1 Maidashi, Higashi-ku, Fukuoka 812-8582, Japan. Phone: 81-92-642-6641. Fax: 81-92-642-6646. E-mail: katayama@phar.kyushu-u.ac.jp.

† These authors contributed equally to this study.

‡ Present address: Institute for Cell and Molecular Biosciences, Medical School, University of Newcastle upon Tyne, Newcastle upon Tyne, United Kingdom.

§ Present address: Shionogi & Co., Ltd., Osaka, Japan.

¶ Present address: Nipro Co., Osaka, Japan.

‖ Present address: Cold Spring Harbor Laboratory, Cold Spring Harbor, NY.

▽ Published ahead of print on 23 May 2008.

the β sliding clamp is required for the RIDA reaction (59). In addition, Hda carries an AAA+ domain (29, 45). AAA+ family proteins, which also include DnaA, share unique motifs associated with functions in nucleotide binding and hydrolysis. The Hda Arg-168 residue in the AAA+ box VII arginine finger motif is required for ATP-DnaA hydrolysis during the RIDA reaction (59). Loss of Hda function increases the level of ATP-DnaA in cells (29). A temperature-sensitive *hda* mutant (*hda-86* mutant) exhibits overinitiation of chromosomal replication from *oriC* at a restrictive temperature, and the excessively formed replication forks stall near the *oriC* (29). Whole-genome microarray analysis demonstrates that *hda*-disrupted cells cause overinitiation of replication from *oriC* (7). The *hda* gene is essential for cell growth, although suppressor mutations can frequently occur, allowing colony formation of *hda* mutants (16, 29, 52).

The *dnaA cos* mutant, a cold-sensitive *dnaA* mutant, exhibits overinitiation of chromosomal DNA from *oriC*, resulting in overreplication of whole chromosomal DNA at a restrictive temperature (30°C) (26, 32). DnaAcos protein is resistant to RIDA and overinitiates the replication of minichromosomes in vitro (23, 25). The function of the *diaA* gene was first identified as a suppressor for the *dnaA cos* mutant (21). Cell division in the *dnaA cos* strain is inhibited in an *sfiA*-independent manner at 30°C (28). SfiA is a member of the SOS-inducible proteins and inhibits the polymerization of FtsZ, arresting cell division (11, 44, 62).

In this study, we have isolated and characterized a novel cold-sensitive *hda* mutant, the *hda-185* mutant which carries an amino acid substitution of K185C. These mutant cells exhibited a more severe inhibition of colony formation than *hda-86* cells did and therefore stimulated the analysis of suppressor mutations. Like the *hda-86* strain, the *hda-185* strain caused overinitiation of chromosomal replication from *oriC* but did not overreplicate the entire chromosomal DNA at 25°C. At this temperature, the levels of DnaA protein and *dnaA* mRNA were comparable to those in the wild-type *hda* strain. Cell division of the *hda-185* strain is inhibited at restrictive temperatures in an *sfiA*-independent manner. Furthermore, we found that multiple copies of the ribonucleotide reductase (RNR) gene increased the deoxyribotrinucleotide (dNTP) levels and repressed overinitiation in the *hda-185* strain.

MATERIALS AND METHODS

Media, bacterial strains, oligonucleotide primers, and plasmids. LB medium contains Bacto tryptone (1%), yeast extract (0.5%), and sodium chloride (1%). Thymine (50 μg/ml) was included in the medium unless indicated otherwise. The bacterial strains and plasmids that were used in this study are listed in Table 1. The sequences of the oligonucleotide primers that were used in this study are listed in Table 2. pTKM103 carries the SacII-NheI chromosomal fragment containing the *dnaB* gene at the corresponding restriction sites on pBR322. pTKM221 carries a promoter region upstream of *nrdH* and the coding region of *nrdEF*. In order to construct this plasmid, the *nrdHIEF* operon was first cloned onto pBR322 using the EcoRI site, resulting in pTKM203. To remove the *nrdHI* coding region from pTKM203, two DNA fragments were amplified by PCR using pTKM203 and two pairs of primers (primers TAKU19 and TAKU25 and primers TAKU20 and TAKU26). The resultant DNA fragments were digested with EcoRI and ClaI and ligated, resulting in pTKM221. The *nrdAB*-carrying DNA fragment was amplified by PCR using the primers TAKU32 and TAKU35; the resultant DNA fragment was cloned into the NheI and HindIII sites of pBR322, resulting in pTKM226. pMS100 was constructed using the QuikChange site-directed mutagenesis kit (Stratagene) with pTKM226 as the template and primers NrdA-1 and NrdA-2. This site-directed mutagenesis method was used throughout this study.

Isolation of cold-sensitive *hda* mutants. In order to screen cold-sensitive *hda* mutants, we utilized incompatibility in ColE1-type plasmids as follows. Plasmids carrying *hda* alleles were constructed by site-directed mutagenesis using pWK21-1 (wild-type *hda* and *kan* genes) and primers (HCS3 and HCS4 for V104N, HCS5 and HCS6 for K185C, HCS7 and HCS8 for R217H, and HCS9 and HCS10 for Q225H). The resultant plasmids were introduced into strain WK001 (Δ*hda*::*cat*) harboring pBAD/Hda (wild-type *hda* and *bla* genes) (59), and colonies were formed on LB plates containing kanamycin (750 μg/ml) at 42°C. Loss of pBAD/Hda was tested in the resultant colonies using LB plates containing ampicillin (100 μg/ml). The selected cells (Kan^r Amp^s) were incubated at 25°C and 30°C on LB plates containing kanamycin (750 μg/ml) in order to assess cold sensitivity. pWK21-1 is a derivative of pBAD/Hda carrying the *kan* gene that was derived from pUC4K and was inserted at the ScaI site within the *bla* gene. Strain WK001 had been constructed previously by P1 transduction using the recipient strain KH5402-1 and a donor strain bearing Δ*hda*::*cat* *dnaA*::*kan* *rnhA*::Tn*3* (29).

Construction of the *hda-185* strain. The DNA fragment containing an *hda* coding region and its upstream (2-kb) and downstream (2-kb) regions was amplified by PCR using genome DNA and the HCS1 and HCS2 oligonucleotides as primers. The resultant fragment was digested with NheI and BamHI and then cloned into pBR322 using the corresponding sites, resulting in pHCS1-1. An *hda* region was amplified by PCR using pHCS1-1 and the HCS12 and HCS13 oligonucleotides as primers. The resultant fragment, together with a kanamycin resistance gene-containing region of DNA, was digested with AscI and NcoI and then ligated, resulting in pHCS2-1. The kanamycin resistance gene had been prepared by PCR using pUC4K and the KM1 and KM2 oligonucleotides as primers. To introduce the mutation *K185C* into *hda* on pHCS2-1, we performed site-directed mutagenesis using pHCS2-1 and the HCS7 and HCS8 oligonucleotides as primers, resulting in pHCS3-1. After digestion with NdeI and BamHI, pHCS2-1 (wild-type *hda*) and pHCS3-1 (*hda-185*) were introduced into strain ME9018 (*recD*::mini-*tet*), and colonies were formed on LB plates containing kanamycin (50 μg/ml) at 42°C. After screening for ampicillin sensitivity, insertion of the kanamycin resistance gene was verified by colony PCR. The kanamycin resistance gene-linked wild-type *hda* gene and *hda-185* were introduced into the MG1655 *thyA rpsL* strain using P1 transduction, resulting in strains YH014 and YH013, respectively.

Construction of *diaA*, *lexA*, *sfiA*, and *slmA* mutants. The wild-type *diaA* in strain MG1655 *thyA rpsL* was replaced with Δ*diaA*::*FRT kan* by P1 transduction using strain JW3118, and the kanamycin resistance gene (*kan*) was removed as described previously (3, 12), resulting in strain YH105 (Δ*diaA*::*FRT*). The *kan*-linked wild-type *hda* or *hda-185* was introduced into strain YH105 by P1 transduction using strain YH014 or YH013, resulting in YH106 or YH107, respectively. The Tn*10*-linked *lexA3* mutation was introduced into YH013 and YH014 using P1 transduction with strain HSR2005. The presence of *lexA3* was verified by UV sensitivity. According to a method described previously (12), the *sfiA* and *slmA* genes in strain MG1655 harboring pKD46 (λ Red expression plasmid) were replaced with a *cat* region that was prepared by PCR using pACYC184 as a template and SFI-1 and SFI-2 oligonucleotides for Δ*sfiA*, and SLM-1 and SLM-2 oligonucleotides for Δ*slmA*. The resultant Δ*sfiA*::*cat* and Δ*slmA*::*cat* were introduced into strains YH013 and YH014, respectively, using P1 transduction.

Determination of the cellular levels of dCTP and dATP. DNA polymerase-based assay for the dCTP level was performed as previously described (63). Briefly, cells were grown in LB medium (10 ml) until an optical density (A_{660}) reached 0.4, collected by centrifugation, and suspended in 60% methanol. The suspension was boiled for 5 min and then centrifuged, and the supernatant was isolated. The sample was dried under vacuum and dissolved in water (20 μl). For analysis of the dCTP level, a portion (0.3 μl) was subjected to a replication assay using [α-^{32}P]dATP, the DNA polymerase I large fragment and a primed DNA template consisting of only thymine and guanine nucleotides.

The level of dATP was determined using two-dimensional thin-layer chromatography as described previously (5) with minor modifications. Briefly, cells were grown at 25°C in modified TG medium containing $^{32}P_i$ (0.4 mCi/ml) (36) until an optical density (A_{660}) reached 0.2. Portions (300 μl) of the cultures were mixed with 30 μl of 11 N formic acid, and supernatants were obtained from the suspension by centrifugation. Portions (1 μl) of the supernatants were mixed with 2 μl of 10 mM dATP and separated on polyethyleneimine-cellulose thin-layer chromatography sheet (Merck). Solvent Tb (0.75 M Tris, 0.45 M HCl, 0.5 M LiCl) and solvent Pb (0.4 M K_2HPO_4, 0.7 M boric acid) were used for the first dimension and second dimension, respectively. The labeled nucleotides were detected using a BAS2500 image analyzer (Fuji Film). The position of dATP was

TABLE 1. List of *E. coli* strains and plasmids used in this study

Bacterial strain or plasmid	Genotype or relevant characteristic(s)	Reference or source
Bacterial strains		
KH5402-1	*ilv thyA tyrA*(Am) *trpE9829*(Am) *metE deo supF6*(Ts)	24
WK001	KH5402-1 Δ*hda*::*cat*	This study
MG1655 *thyA rpsL*	*ilvG rfb rph thyA rpsL*	J. Kato[a]
YH014	MG1655 *thyA rpsL hda*$^+$ *kan*	This study
YH013	MG1655 *thyA rpsL hda-185 kan*	This study
KA413	KH5402-1 *dnaA46 ilv*$^+$	24
NA001	KH5402-1 *dnaA cos*	24
ME9018	MG1655 *recD1903*::mini-*tet*	NIG[b]
KA483	KH5402-1 *seqA*::Tn*10 zid-131*::Tn*5*	This study
KA470	KH5402-1 *zid-16T*::Tn*10*	This study
NA169	KH5402-1 *recA*::Tn*10*	21
KW262	MG1655 *rnhA*::Tn*3* Δ*oriC*::*tet*	29
MK86	KW262 Δ*hda*::*cat*	29
JW3118	BW25113 Δ*diaA*::*FRT kan*	3[c]
YH105	MG1655 *thyA rpsL* Δ*diaA*::*FRT*	This study
YH106	YH105 *hda*$^+$ *kan*	This study
YH107	YH105 *hda-185 kan*	This study
MZ002	YH014 Δ*sfiA*::*cat*	This study
MZ001	YH013 Δ*sfiA*::*cat*	This study
HSR2005	AB1157 except for *lexA3*::Tn*10*	55[d]
YH101	YH014 *lexA3*::Tn*10*	This study
YH102	YH013 *lexA3*::Tn*10*	This study
YH103	YH014 Δ*slmA*::*cat*	This study
YH104	YH013 Δ*slmA*::*cat*	This study
KP7364	KP245 Δ*dnaA*::*spec rnhA*::*kan*	36
Plasmids		
pBR322	*tet bla*	Laboratory stock
pACYC177	*bla kan*	Laboratory stock
pACYC184	*cat tet*	Laboratory stock
pUC4K	*kan bla*	Laboratory stock
pWK21-1	ColE1*ori* P_{BAD} *hda kan*	This study
pBAD/Hda	ColE1*ori* P_{BAD} *hda bla*	59
pYHM1	pWK21-1 except for *hda* V104N substitution	This study
pYHM2	pWK21-1 except for *hda* K185C substitution	This study
pYHM3	pWK21-1 except for *hda* R217H substitution	This study
pYHM4	pWK21-1 except for *hda* Q225H substitution	This study
pHCS1-1	pBR322-*hda* and adjacent region	This study
pHCS2-1	pHCS1-1 except for carrying *kan* downstream of *hda*	This study
pHCS3-1	pHCS2-1 except for *hda* K185C substitution	This study
pHCS4-1	pACYC177-*hda*	This study
pTKM221	pBR322-*nrdEF*	This study
pTKM226	pBR322-*nrdAB*	This study
pTKM103	pBR322-*dnaB*	This study
pMS100	pTKM226 except for *nrdA* C439A substitution	This study
pTSO182	pBR322-*oriC*	26

[a] Gift from J. Kato.
[b] NIG, National Institute of Genetics, Japan.
[c] National BioResource Project of Japan.
[d] Gift from T. Hishida.

determined by UV absorbance. The positions of ATP and GTP were determined by the method of Bochner and Ames (5).

Determination of the *oriC*/*terC* ratio by Southern blotting and a quantitative PCR method. The dosage of the *oriC* and *terC* genes in cells was measured by Southern blotting or a quantitative PCR method. Chromosomal DNA from the cells was prepared following a standard protocol. Southern blot analysis was performed essentially as described previously (47) except the chromosomal DNA was digested with StyI and EcoRI, and *oriC* and *terC* probes were amplified using chromosomal DNA as a template and primers ORI_1 and ORI_2 for the *oriC* probe and primers TER_1 and TER_2 for the *terC* probe. These probes were labeled using the Megaprime DNA labeling system (Amersham) and [α-^{32}P]dCTP. Quantitative PCR was performed according to the manufacturer's instructions (Takara Bio). Sybr Premix *Ex Taq* (Takara Bio) was used for each reaction to amplify and quantify the *oriC* and *terC* regions. The reaction mixtures (25 μl) contained chromosomal DNA (1 ng) and primers (5 pmol each) (primers ORI_1 and KWoriCRev for *oriC*; primers SUEterFw1 and TER_2 for *terC*). The amplification and quantification were carried out using the Thermal Cycler Dice real-time system (Takara Bio). The *oriC*/*terC* ratio was normalized using strain KA413 (*dnaA46*) incubated at 42°C for 2 h.

Measurement of DNA synthesis. DNA synthesis was measured as described previously (28). Whole chromosomal DNA was labeled while the cells were growing in LB medium containing [^{3}H]thymine (25 μg/ml, 3 μCi/ml). The cells were withdrawn and kept on ice for at least 15 min in the presence of trichloroacetic acid (7%). Insoluble materials were collected on a GF/C filter (Whatman), and [^{3}H]thymine incorporation was quantified using a liquid scintillation counter.

Measurement of DnaA content. DnaA content in the cells was determined by immunoblot analysis using an anti-DnaA antibody as described previously (30, 31). Briefly, aliquots (200 μl at an A_{660} of 0.1) of the cells were collected during exponential growth, immediately transferred to chilled trichloroacetic acid

TABLE 2. List of oligonucleotide primers used in this study

Oligonucleotide primer	Sequence
HCS1	CTAGCTAGCGCGTGAGCAAGATATCAGCAC
HCS2	CGCGGATCCCAATTCGGTTAAGACACCG
HCS3	GCGCACGCTATTTATGACGTTGGATCACCTCGATCGTGCG
HCS4	CGCACGATCGAGGTGATCCAACGTCATAAATAGCGTGCGC
HCS5	GCGGCTCGACAGAGAAATGCACACGCTATTTATGACGTTGG
HCS6	CCAACGTCATAAATAGCGTGTGCATTTCTCTGTCGAGCCGC
HCS7	GCCACTTTCTGATGAAGATTGCCTGCAGGCGCTACAGTTACGC
HCS8	GCGTAACTGTAGCGCCTGCAGGCAATCTTCATCAGAAAGTGGC
HCS10	CCTGGTTTGTTCCGGAAAACCTCGACGGTATGGAGC
HCS11	GCTCCATACCGTCGAGGTTTTCCGGAACAAACCAGG
HCS12	CATGCCATGGCATAGTATTCGTAGGCCGG
HCS13	GGCGCGCCGATTAACTTCGCGTAGTTCG
ORI_1	CTGTGAATGATCGGTGATCC
ORI_2	AGCTCAAACGCATCTTCCAG
TER_1	CAGAGCGATATATCACAGCG
TER_2	TATCTTCCTGCTCAACGGTC
KM1	GGCGCGCCTTGTCGGGAAGATGCGTG
KM2	CATGCCATGGGGGAAAGCCACGTTGTGTC
TAKU19	GGAATTCCGTGGCACTGAACGCAATC
TAKU20	GGAATTCGCTGTACCGTTTTGAACTCATGG
TAKU25	GCTTAATTCGTAAAACCCCTGGCTTCGG
TAKU26	CGACATGAGAGAGCAACTCGCTAAGAGGC
TAKU32	CTAGCTAGCGGAGCCAATCCCCAAAGC
TAKU35	CCCAAGCTTCTTGCAAGAGGGTCATTTTC
NrdA-1	GCGTCAGTCTAACCTGGCGCTGGAGATAGCCCTG
NrdA-2	CAGGGCTATCTCCAGCGCCAGGTTAGACTGACGC
KWoriCRev	GTGGATAACTCTGTCAGGAAGCTTG
SUEterFw1	AACTACGCGGGAAATACCC
SFI-1	CGACTGAAAGCATTGGCTGGGCGACAAAAAAAGTTCCAGGATTAATCCTAGA GAGCCTGAGCAAACTG
SFI-2	ATCATAACATAAAAGAATGATTCACATTAACGGATCCGTTAACTACGAAACC AAACCTGTGACGGAAGATCAC
SLM-1	AATAACGTCATAACATAGCCGCAAACATTTCGTTTGCGGTCATAGCGTGGCCT GTGACGGAAGATCAC
SLM-2	AGTTTGGCGTTTAAAGAAACTCGCCGGATGAAAAGTCATCCGGCGTCATAGA GAGCCTGAGCAAACTG
R-dnaA1	GAGTCCGCCGTGTCACTTTC
R-dnaA2	CAATGGGCGTATCCACATACTG
R-rpoA1	TTGATATCGAGCAAGTGAGTTCG
R-rpoA2	GCATCGATGAGAGCAGAATACG

(10%), and kept on ice for at least 15 min. Precipitates were collected by centrifugation, dissolved in sodium dodecyl sulfate (SDS) sample buffer, and separated by 10% SDS-polyacrylamide gel electrophoresis (PAGE). Purified DnaA mixed with a whole-cell extract of strain KP7364 (Δ*dnaA*) was also used for a standard. The proteins were transferred to a polyvinylidene difluoride membrane (Immobilon-P; Millipore) using a semidry blotting method.

Flow cytometry analysis. The flow cytometry experiment was performed as described previously (31, 33). To determine the number of *oriC* in cells, the cells were exponentially grown for 10 generations until the optical density (A_{660}) reached 0.1 to 0.2, and then rifampin (300 μg/ml) and cephalexin (10 μg/ml) were added. After further incubation for 4 h to complete ongoing replication, the cells were fixed in 70% ethanol. The fixed cells were washed and stained with 2 μM Sytox green (Invitrogen), followed by analysis using a FACSCalibur (Becton Dickinson). To determine the cell mass and DNA content, cells that were in the exponential growth phase were incubated in 70% ethanol, washed, and suspended in buffer as described above, followed by analysis using a FACSCalibur.

Quantification of the *dnaA* mRNA level. Total cellular RNA was isolated by the hot phenol method (50). Quantitative reverse transcription-PCR (RT-PCR) was performed using the One Step SYBR PrimeScript RT-PCR kit and Thermal Cycler Dice real-time system (Takara Bio). The reaction mixtures (25 μl) contained DNase I-treated total RNA (1 ng) and primers (5 pmol each) (primers R-dnaA1 and R-dnaA2 for *dnaA* mRNA; primers R-rpoA1 and R-rpoA2 for *rpoA* mRNA). An S1 nuclease assay was performed as described previously (58). The *dnaA* probe (5′-CGGGCAAGACACTGCTGCCAAAGCGAAAGTGAC ACGGCGGACTCCCAGATCCACC-3′) and the *rpoA* probe have been described previously (60) and were end labeled with ^{32}P. After hybridization of these probes with total RNA and S1 nuclease digestion, the products were analyzed using 8 M urea–10% PAGE and quantified with a BAS2500 image analyzer (Fuji Film).

RESULTS

Construction of a cold-sensitive *hda* mutant. We had previously isolated several cold-sensitive *dnaA* mutants bearing the single-amino-acid substitutions I219N, R302C, R334H, and R342H (19). These mutations reside in the AAA+ domain which is shared by DnaA and Hda. Indeed, Hda carries the same residues or residues that are chemically similar to those in DnaA (Fig. 1). We therefore speculated that substitutions in Hda that were identical to those resulting in cold-sensitive *dnaA* mutants might also render Hda cold sensitive. By site-directed mutagenesis, we introduced these substitutions in the *hda* allele carried on a kanamycin-resistant plasmid derived from ColE1. The resultant plasmids carrying an *hda* mutation (V104N, K185C, R217H, or Q225H) were introduced into the chromosomal *hda*-deleted strain bearing a wild-type *hda* gene on an ampicillin-resistant plasmid derived from ColE1. The transformed cells that were resistant to kanamycin and sensi-

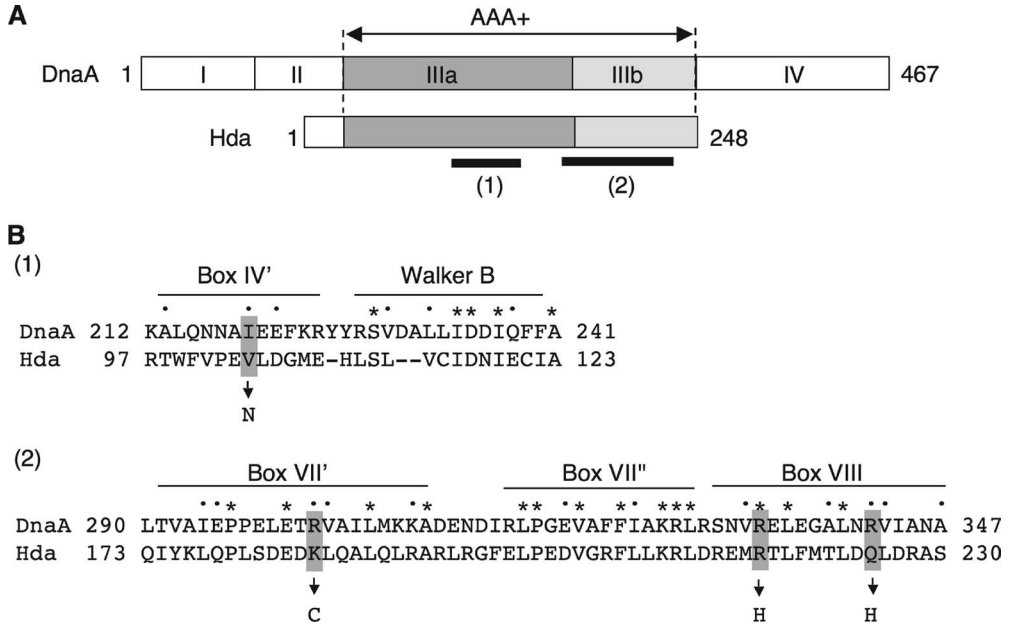

FIG. 1. Structure of DnaA and Hda and the mutation sites. (A) Domain structure of *Escherichia coli* DnaA and Hda. These proteins share a homologous region called the AAA+ domain (15, 29, 59). DnaA has four functional domains (I to IV); domain III (AAA+) has IIIa and IIIb subdomains. The amino acid sequences of the indicated regions [black bars labeled (1) and (2)] are shown in panel B. (B) Amino acid substitutions in cold-sensitive DnaA mutants (19) and in Hda mutants constructed in this study are indicated. Identical (*) and chemically similar (.) residues in DnaA and Hda are also shown.

tive to ampicillin were then selected at 42°C and tested for colony formation at 42°C, 30°C, or 25°C (Table 3). Moderate inhibition of colony formation was observed for the *hda-185* (K185C) mutant at 25°C. We next replaced the *hda* gene on the chromosome with the *hda-185* allele (see Materials and Methods for details). The resultant strain, YH013, exhibited cold sensitivity during colony formation (Table 4). This cold-sensitive colony formation was complemented by a plasmid bearing the wild-type *hda* gene (pHCS4-1) to a level that was comparable to that of the wild-type strain (Table 4), confirming that cold sensitivity depends on the *hda* mutation.

Overinitiation of replication in the *hda-185* mutant. We next asked whether the *hda-185* strain causes the overinitiation of chromosomal replication at 25°C. The copy number ratio of *oriC* to *terC* (replication termination region) was analyzed using Southern blot hybridization (Fig. 2A). The *ori*/*ter* ratio increased upon the temperature shift down to 25°C in the *hda-185* strain but not in the wild-type control strain, suggesting that overinitiation occurs in the *hda-185* strain at this temperature. Consistent with the previous observations in *hda-86* mutants (29), overall chromosomal DNA synthesis did not increase in the *hda-185* strain after the shift to 25°C (Fig. 2B), which suggests that the progression of replication forks is blocked near *oriC* in these mutants. Reduction of overall DNA synthesis was not significantly observed at 25°C even in the *hda-185* strain (Fig. 2B), which suggests that overinitiation indeed occurred and that the replication fork block was not the only cause of the increase in the *oriC*/*ter* ratio. In this experiment, the *dnaA cos* mutant, which causes overreplication of the entire chromosome (32), was also used for comparison.

For an independent approach, we performed flow cytometry experiments (Fig. 2C). Cells were exponentially grown at 42°C, transferred to 25°C, and incubated for 2 h at 25°C, followed by further incubation at 42°C for 4 h in the presence of rifampin and cephalexin. If the *hda-185* cells cause overinitiation at 25°C and the resultant blocked replication forks are reactivated and proceed during incubation at 42°C, the overall DNA content should have increased. After incubation at 25°C for 2 h, the DNA content observed was basically similar to the DNA contents of the wild-type and *hda-185* cells (Fig. 2C), consistent with the data of Fig. 2B. Only a small population of the *hda-185* cells showed DNA contents equivalent to eight or more chromosomes. After subsequent incubation at 42°C for 4 h, overall DNA contents in the *hda-185* cells were evidently higher at 42°C than those in the wild-type cells (Fig. 2C). In

TABLE 3. Colony formation ability of cells bearing a mutant *hda* allele[a]

Amino acid substitution on *hda* allele on plasmid	CFU/ml (10^9) for cells grown at the following temp:			Ratio of CFU/ml for cells grown at the following temp:	
	42°C	30°C	25°C	30°C/42°C	25°C/42°C
None (wild type)	1.3	1.2	1.3	1.0	1.0
V104N	1.1	0.5	0.24	0.45	0.22
K185C	1.0	0.084	1.0×10^{-3}	0.084	1.0×10^{-3}
R217H	1.3	1.3	1.3	1.0	1.0
Q225H	1.1	0.68	0.17	0.62	0.15

[a] WK001 (Δ*hda*) cells harboring a plasmid carrying wild-type *hda* or the indicated mutant allele were grown overnight in LB medium at 42°C. These cells were incubated on LB plates at 42°C for 12 h, at 30°C for 18 h, or at 25°C for 27 h. Kanamycin (750 μg/ml) was included in the medium, with the exception of the medium for WK001 cells carrying the wild-type *hda*-plasmid when ampicillin (100 μg/ml) was included.

TABLE 4. Colony formation ability of cells bearing an *hda-185* allele[a]

Strain	Relevant genotype	CFU/ml (10^9) for cells grown at the following temp:			Ratio of CFU/ml for cells grown at the following temp:	
		42°C	30°C	25°C	30°C/42°C	25°C/42°C
MG1655 *thyA rpsL*	*hda*$^+$	1.0	1.0	1.1	1	1.1
YH014	*hda*$^+$ *kan*	2.7	2.7	2.8	1	1
YH013	*hda-185 kan*	1.7	1.0×10^{-3}	2.0×10^{-4}	5.9×10^{-4}	1.2×10^{-4}
YH013/pACYC177	*hda-185*	2.6	1.0×10^{-3}	2.0×10^{-4}	3.8×10^{-4}	7.7×10^{-5}
YH013/pHCS4-1	*hda-185*	2.6	3.0	2.8	1.2	1.1
YH014/pACYC177	*hda*$^+$	1.9	1.8	1.8	0.95	0.95
YH014/pHCS4-1	*hda*$^+$	2.3	2.6	2.3	1.1	1

[a] Cells from the indicated strains were grown overnight at 42°C and incubated on LB plates at 42°C for 12 h, at 30°C for 18 h, or at 25°C for 27 h. The medium contained kanamycin (50 μg/ml) for strains YH013 and YH014. Ampicillin (100 μg/ml) was included when a plasmid (pACYC177 vector or pHCS4-1) was present. pHCS4-1 is a derivative of pACYC177 carrying wild-type *hda* (*hda*$^+$).

wild-type cells, run-out replication at 42°C yielded four or eight chromosomes per cell and cells containing four chromosomes were predominant (Fig. 2C). In the *hda-185* mutant, cells showing a DNA content equivalent to eight chromosomes were most abundant, and a considerable population of cells showed further elevated DNA contents. Discrete peaks of DNA histograms were not formed for these cells, which suggest that some replication forks were stalled or severely retarded even at 42°C and could not replicate whole chromosomal DNA. Similar results were obtained when the cells were incubated in the presence of chloramphenicol in addition to rifampin and cephalexin after a shift to 42°C (data not shown). A similar cell mass was observed for the wild-type and *hda-185* cells after incubation at 25°C for 2 h (Fig. 2C). At this time range, inhibition of cell division did not occur in the *hda-185* cells (see below). These results support the idea that overinitiation occurs at 25°C in *hda-185* cells.

A similar analysis was performed using *hda-185* cells grown at 42°C. These cells were incubated in the presence of rifampin and cephalexin. DNA histograms showed a broad distribution in chromosome equivalents of up to eight or more (data not shown), indicating that the negative regulation of initiation is not complete even at 42°C.

DnaA molecules are not oversupplied in *hda-185* cells. Western blot analysis revealed that the cellular contents of DnaA protein in *hda-185* cells were similar at 25°C to those in the wild-type control strain (Fig. 2D). In both strains, a slight increase in the contents might be present after a temperature shift from 42°C, but at 25°C the overall levels in the both strains were similar. These results indicate that overinitiation in the *hda-185* strain is independent of the DnaA dosage.

***dnaA* transcription level in *hda*-deficient strains.** *dnaA* transcription is autoregulated by DnaA protein, and the nucleotide forms of DnaA affect its repressor activity in vitro (57). We used real-time PCR to quantitatively examine whether the defects in *hda* could affect the *dnaA* transcription level (Fig. 3). We first measured the *dnaA* mRNA levels in *hda-185* cells at 42°C and 25°C using the *rpoA* mRNA as a normalization control (Fig. 3A). At 25°C, the *dnaA* mRNA levels in the wild-type *hda* cells and *hda-185* cells were comparable. After a temperature shift down from 42°C, the *dnaA* mRNA level might be slightly increased, which is consistent with the result of the cellular DnaA contents in response to a similar temperature change (Fig. 2D).

We also measured the *dnaA* mRNA levels in Δ*oriC* Δ*rnhA* mutants bearing the wild-type *hda* or Δ*hda* allele. Chromosomal replication in the Δ*rnhA* mutant occurs in a manner independent of DnaA and *oriC* (29, 35). The *dnaA* mRNA levels in the wild-type *hda* cells and Δ*hda* cells were comparable (Fig. 3B). These results are consistent with the idea that *hda* did not significantly affect *dnaA* transcription.

The growth defect in the *hda-185* strain is stimulated by disruptions in *seqA* or *recA*. SeqA preferentially binds to hemimethylated *oriC* DNA and represses the initiation at *oriC* (38, 46, 56). We performed P1 transduction using Δ*seqA*::Tn*10*. Transduction into the *hda-185* mutant was severely inhibited even at 42°C, unlike control transductions using the wild-type strain as a recipient or using Δ*zid-16T*::Tn*10* as a donor (Table 5). These results suggest that overinitiation of replication in *hda-185* cells is not completely repressed even at 42°C, consistent with flow cytometry analysis using the *hda-185* cells grown at 42°C. Most likely the SeqA function, which acts in an RIDA-independent manner, is required for inhibiting severe overinitiation and for rescuing cell growth.

Stalled replication forks can lead to double-strand breaks, which if they are not repaired, cause cell death (17). RecA is responsible for double-strand break repair (9). We found that P1 transduction using Δ*recA*::Tn*10* into the *hda-185* strain was severely inhibited even at 42°C (Table 5); this result is in contrast to that obtained using the *dnaA cos* mutant (28). RecA-dependent recombination might be required for the stalled fork repair in the *hda-185* cells.

Growth of the *hda-185* strain is rescued by disruption of the *diaA* gene and the multicopy *oriC*. When an *oriC* plasmid was introduced into the *hda-185* strain, cell growth at 25°C was restored (Table 6); this result is similar to that observed with the *dnaA cos* mutant (26). In addition, cells bearing *hda-185* and Δ*diaA* double mutations exhibited colony formation at 25°C in a manner similar to that of the control wild-type *hda* strain (Table 6). This is consistent with the previous observation that *diaA* deletion suppresses the growth defect in the *dnaA cos* mutant cells (21) and in cells expressing the ATP hydrolysis-defective mutant of DnaA, DnaA R334A (33). Taken together, these results support the idea that the *hda-185* mutant causes overinitiation due to an elevated level of DnaA activity.

Elevated ATP-DnaA level in the *hda-185* Δ*diaA* cells. In a culture of wild-type cells, the ATP-DnaA level is repressed to

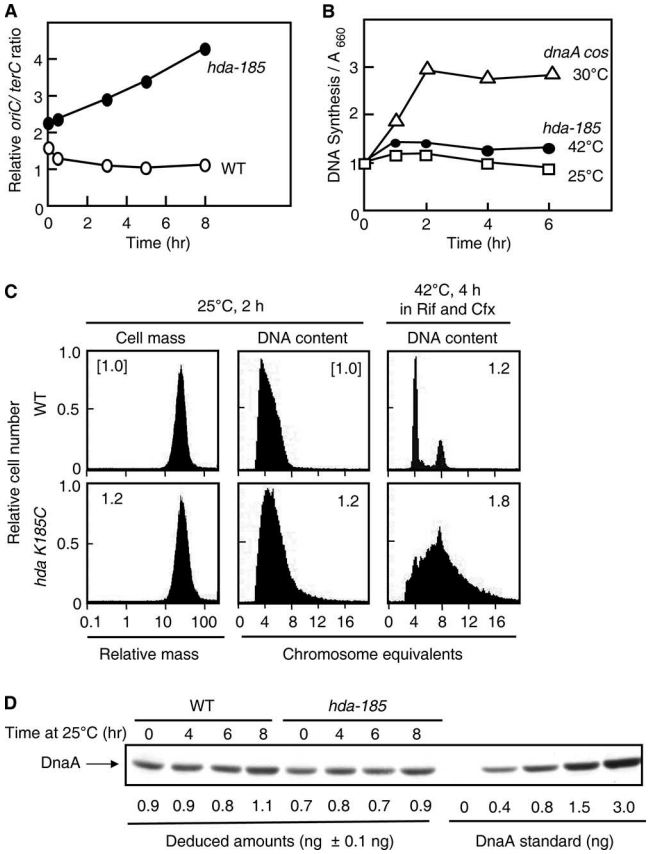

FIG. 2. *oriC*/*terC* ratio, DNA synthesis, and DnaA content in the *hda-185* cells. (A) Ratio of *oriC* per *terC*. Gene dosages of *oriC* and *terC* were determined by Southern blot analysis using a probe specific to *oriC* or *terC*, respectively. Cells from strain YH014 (wild-type *hda* [WT]) or YH013 (*hda-185*) were grown at 42°C in LB medium until the optical density (A_{660}) reached 0.1, diluted, and further incubated at 25°C. At the indicated time (in hours) from the temperature shift, portions were withdrawn, and the samples were subjected to Southern blot analysis as described in Materials and Methods. The *oriC*/*terC* ratio was normalized to strain KA413 (*dnaA46*) incubated at 42°C for 2 h. (B) Chromosomal DNA synthesis. YH013 (*hda-185*) and NA001 (*dnaA cos*) cells were grown at 42°C in LB medium containing [^{3}H]thymine until the optical density (A_{660}) reached 0.1 and further incubated for the indicated times at 25°C or 42°C for strain YH013 or at 30°C for strain NA001. Relative ratios of incorporated thymine per the optical density of the culture are shown. The value at time zero was defined as 1. Incorporated ^{3}H at time zero in the deduced samples (0.5 ml) was 1.3×10^4 and 1.4×10^4 cpm for YH013 and NA001, respectively. (C) Flow cytometry analysis. YH014 (WT) and YH013 (*hda-185*) cells were grown at 42°C, followed by incubation at 25°C for 2 h and analysis using flow cytometry (25°C, 2 h). Some cells were further incubated at 42°C for 4 h in the presence of rifampin and cephalexin, followed by flow cytometry analysis (42°C, 4 h in Rif and Cfx). Relative cell mass and DNA contents were measured as described in Materials and Methods. The mean cell mass and mean DNA content of YH014 cells incubated at 25°C for 2 h are defined as 1, and relative values are shown. (D) Cellular DnaA contents. Immunoblot analysis was performed using an anti-DnaA antibody as described in Materials and Methods. YH014 (WT) or YH013 (*hda-185*) cells were incubated as described above for panel A. Portions of the culture (200 μl at an A_{660} of 0.1) or portions including the total cell volume equivalent to this were used for SDS-PAGE and immunoblot analysis. Purified DnaA was used for a quantitative standard.

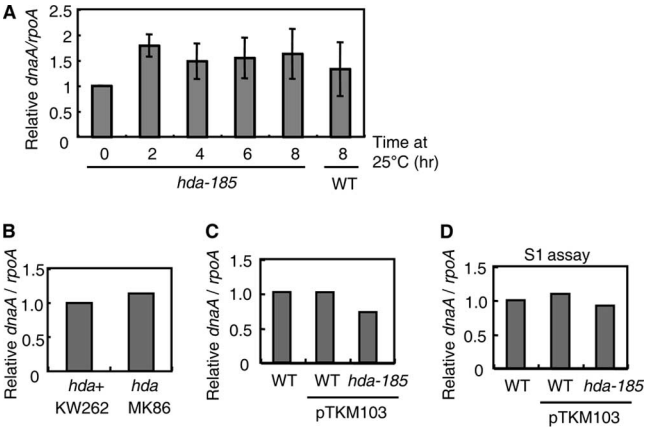

FIG. 3. Quantification of the *dnaA* mRNA level. A quantitative RT-PCR (A to C) and a quantitative S1 nuclease assay (D) were performed as described in Materials and Methods. In these experiments, the *rpoA* mRNA level was used as an internal quantitative control. (A) Relative *dnaA* mRNA levels in strains YH014 (wild-type *hda* [WT]) and YH013 (*hda-185*). Cells of these strains were grown at 42°C, shifted to 25°C, and incubated for the indicated times (in hours) as described in the legend to Fig. 2A. Total RNA was isolated from the cells and used for the RT-PCR analysis of *dnaA* and *rpoA* mRNA levels. Four measurements were performed, and standard deviations are also shown. (B) Relative *dnaA* mRNA levels in the *hda*-null strain. Total RNA was isolated from KW262 (*rnh*::Tn*3* Δ*oriC*::*tet*) (*hda*$^+$) and MK86 (*rnh*::Tn*3* Δ*oriC*::*tet* Δ*hda*::*cat*) (*hda* mutant) cells that were grown at 37°C until the optical density (A_{660}) reached 0.4. (C and D) *dnaA* mRNA level in DnaB-oversupplied cells. Cells of strain YH014 (WT), YH014 carrying pTKM103 (*dnaB*), and YH013 (*hda-185*) carrying pTKM103 were grown at 25°C until the optical density (A_{660}) reached 0.5. Total RNA was isolated, and the relative *dnaA* mRNA levels were analyzed by RT-PCR (C) or S1 nuclease assay (D).

about 20% of total ATP/ADP-DnaA molecules in a manner dependent on *hda* and DNA replication (29, 36). We attempted to assess the in vivo nucleotide forms of DnaA in *hda-185* cells by ^{32}P labeling and immunoprecipitation as we have done previously (27, 29, 36); however, growth of the *hda-185* cells was severely inhibited in a phosphate-limited minimum medium which is required for ^{32}P labeling (data not shown). Similar growth inhibition was also observed for the *hda-86*(Ts) cells but not for the cells bearing disruptions in the *hda*, *oriC*, and *rnhA* genes (29). The *hda-185* cells and *hda-86* cells would have residual levels of overinitiation even at permissive temperatures (Table 5) (29), which could be related to the growth inhibition in the medium.

Unlike the *hda-185* cells, the *hda-185* Δ*diaA* double mutant cells could grow in the phosphate-limited medium at a rate similar to those of the wild-type cells and Δ*diaA* cells. When these cells were grown at 25°C, the ATP-DnaA level in the *hda-185* Δ*diaA* cells was about twofold higher than the level in the wild-type cells (Fig. 4). The ATP-DnaA level in the Δ*diaA* cells might be only slightly higher than that in the wild-type cells. These results indicate that *hda-185* is dysfunctional at 25°C and suggest that overinitiation is caused in the presence of the wild-type *diaA* by the elevated level of ATP-DnaA.

In our previous study, the ATP-DnaA level increased up to 70% to 80% depending on inhibition of DNA replication or disruption of *hda* at 37°C or 42°C (29, 36, 51). In the present study, the cellular ATP-DnaA level was increased up to 39% at

TABLE 5. Effect of the combination of *hda-185* with a disruption in *seqA* or *recA*[a]

Donor strain genotype	Recipient strain	Transduction frequency (42°C)[b]	Relative efficiency[c]
zid-16T::Tn*10*	MG1655 *thyA rpsL* (*hda*$^+$)	5.9×10^{-7}	1
	YH014 (*hda*$^+$)	2.6×10^{-7}	0.44
	YH013 (*hda-185*)	2.9×10^{-8}	4.9×10^{-2}
Δ*seqA*::Tn*10*	MG1655 *thyA rpsL* (*hda*$^+$)	1.4×10^{-8}	2.4×10^{-2}
	YH014 (*hda*$^+$)	1.7×10^{-8}	2.8×10^{-2}
	YH013 (*hda-185*)	$<7.5 \times 10^{-11}$	$<1.3 \times 10^{-4}$
Δ*recA*::Tn*10*	MG1655 *thyA rpsL* (*hda*$^+$)	27×10^{-7}	0.45
	YH014 (*hda*$^+$)	2.4×10^{-7}	0.41
	YH013 (*hda-185*)	$<6.7 \times 10^{-10}$	$<1.1 \times 10^{-3}$

[a] P1 transduction was performed using P1*vir* phages propagated in strain KA470 for *zid-16T*::Tn*10*, strain KA483 for *seqA*::Tn*10*, and strain NA169 for *recA*::Tn*10*. The recipient strains and their relevant genotypes are indicated. Colonies of transductants were counted after incubation at 42°C for 12 h on LB plates. These plates contained tetracycline (15 μg/ml) and kanamycin (50 μg/ml) for strains YH014 and YH013 or tetracycline (15 μg/ml) for strain MG1655 *thyA rpsL*. The *zid-16T*::Tn*10* strain was used as a positive control.

[b] The transduction frequency is the number of transductant colonies per P1 phage.

[c] Efficiency relative to the transduction frequency of the *zid-16T*::Tn*10* strain for MG1655 *thyA rpsL*.

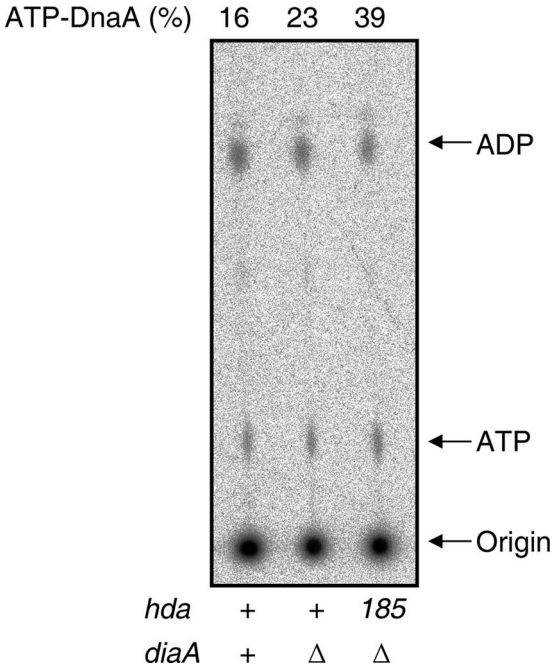

FIG. 4. The ATP-DnaA level in Δ*diaA hda-185* cells. Strain YH014 (*hda*$^+$ *diaA*$^+$), YH106 (*hda*$^+$ Δ*diaA*), and YH107 (*hda-185* Δ*diaA*) cells were grown exponentially at 25°C in the presence of $^{32}P_i$ in modified TG medium (36). Nucleotide-bound DnaA protein was immunochemically isolated from cell lysates, and the recovered nucleotides were analyzed as described previously (36). The proportions (as percentages) of ATP-DnaA in the total ATP/ADP-DnaA are shown above the plate. The migration positions of ATP and ADP are indicated to the right of the plate.

25°C (Fig. 4), a lower level than above. This might be caused by a residual activity of Hda-185 or moderated production of ATP-DnaA at low temperatures.

Oversupply of DnaB or RNRs suppresses the cold-sensitive growth of the *hda-185* mutant. We have previously isolated multicopy suppressors for the *dnaA cos* strain using a DNA library containing chromosomal fragments cloned into pBR322 (28). Restriction enzyme analysis distinguishes these suppressor plasmids into seven groups (group A and groups C to H) (28). Deletion analyses of plasmids in groups D and F revealed that the *dnaB* gene and the *nrdEF* genes are responsible for the *dnaA cos* suppression, respectively (T. Ishida and T. Katayama, unpublished data). Notably, we found that pBR322 carrying either the *dnaB* gene or the *nrdEF* genes also suppresses cold-sensitive colony formation in the *hda-185* mutant (Table 6). The presence of excessive numbers of DnaB molecules in the *hda-185* mutant might abnormally interact with DnaA, resulting in the inhibition of overinitiation (see below).

The *nrdEF* operon and the *nrdAB* operon encode an RNR that functions at a rate-limiting step for synthesizing dNTPs. NrdAB is the major RNR, and NrdEF is an alternative enzyme that is expressed under specific conditions (48). When we in-

TABLE 6. Effects of deletion of *diaA* and multicopy supply of *oriC*, *dnaB*, *nrdAB*, and *nrdEF*[a]

Strain	Relevant genotype	CFU/ml (10^9) for cells grown at the following temp:		Ratio of CFU/ml for cells grown at 25°C/42°C
		42°C	25°C	
YH014	*hda*$^+$	4.3	4.6	0.9
YH013	*hda-185*	3.8	1.4×10^{-3}	3.7×10^{-4}
YH106	*hda*$^+$ Δ*diaA*::*FRT*	1.9	1.8	1.0
YH107	*hda-185* Δ*diaA*::*FRT*	2.1	2.2	1.0
YH014/pBR322	*hda*$^+$	1.9	1.6	0.84
YH013/pBR322	*hda-185*	2.6	<0.001	$<3.8 \times 10^{-4}$
YH014/pTSO182 (*oriC*)	*hda*$^+$	1.7	1.6	0.94
YH013/pTSO182 (*oriC*)	*hda-185*	1.4	0.9	0.64
YH013/pTKM103 (*dnaB*)	*hda-185*	1.7	1.8	1.1
YH013/pTKM226 (*nrdAB*)	*hda-185*	2.5	2.8	1.1
YH013/pTKM221 (*nrdEF*)	*hda-185*	2.3	1.6	0.7
YH013/pMS100 [*nrdA*(C439A) *nrdB*$^+$]	*hda-185*	1.9	<0.002	$<1.1 \times 10^{-3}$

[a] Cells of the indicated strains were grown overnight in LB medium at 42°C and then incubated on LB plates at 42°C for 12 h or at 25°C for 27 h. Ampicillin (100 μg/ml) was included when plasmids were present.

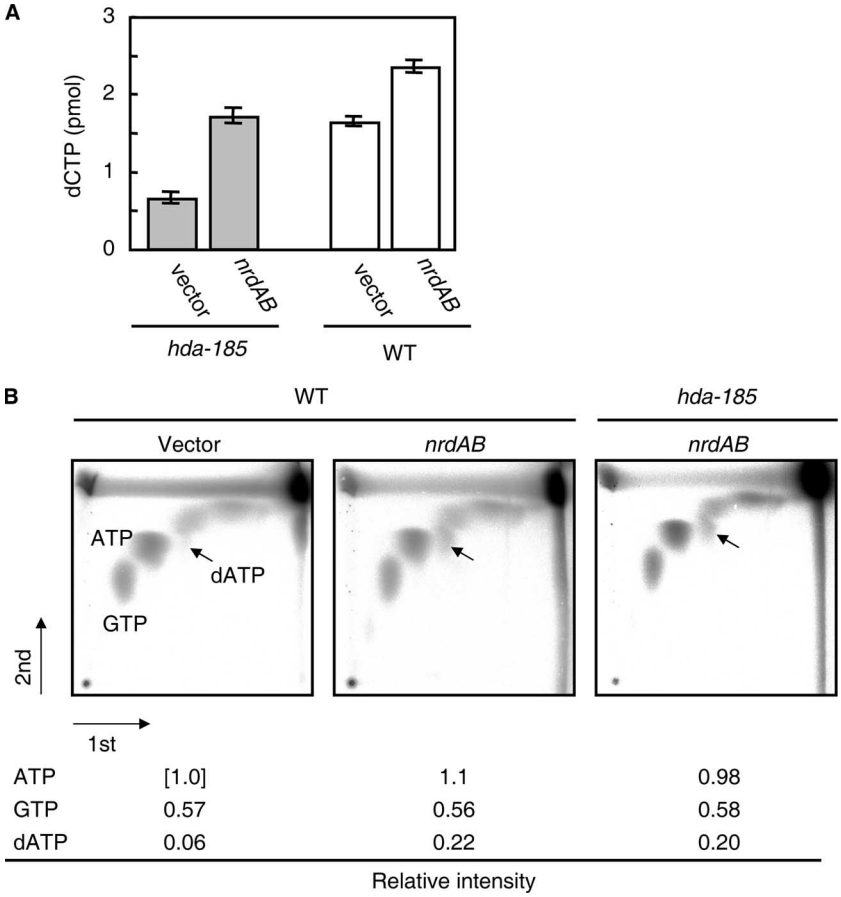

FIG. 5. Effect of multiple copies of *nrdAB* on dNTP pools. (A) Cellular dCTP levels. The cellular levels of dCTP pool were determined using a DNA polymerase-dependent assay as described by Wheeler et al. (63). YH014 (wild-type *hda* [WT]) or YH013 (*hda-185*) cells carrying the indicated plasmid (vector, pBR322; *nrdAB*, pTKM226) were grown at 42°C and further incubated at 25°C for 8 h. Methanol-soluble extracts were prepared from the cells and assessed for dCTP using the DNA polymerase I large fragment and [α-^{32}P]dATP. The dCTP contents were deduced using a standard dCTP solution. Duplicated samples were assessed, and standard deviations (error bars) are shown. (B) Cellular dATP levels. The cellular dATP level was determined using two-dimensional thin-layer chromatography as described in Materials and Methods. YH014 (WT) or YH013 (*hda-185*) cells carrying the indicated plasmid (vector, pBR322; *nrdAB*, pTKM226) were exponentially grown at 25°C in modified TG medium containing ampicillin and $^{32}P_i$. Nucleotides contained in an equivalent cell volume of the samples were extracted in formic acid, separated using two-dimensional thin-layer chromatography, and visualized by using a BAS2500 image analyzer (Fuji Film). The relative intensities of the spots corresponding to ATP, GTP, and dATP are also shown. The intensity of ATP of strain YH014 carrying pBR322 is defined as 1. The position of dATP is indicated by an arrow on each sheet.

troduced pBR322 carrying the *nrdAB* genes into the *hda-185* strain, suppression of cold sensitivity was also observed (Table 6). The Cys-439 residue within NrdA is located in the catalytic pocket in which the substrates bind and is essential for RNR activity (2, 13). The NrdA C439A mutant protein exhibits no enzymatic activity in vivo or in vitro, whereas the stability of the protein is not affected (2, 13). pBR322 bearing *nrdA* C439A and wild-type *nrdB* was impaired in *hda-185* suppression activity (Table 6). These results support the idea that an active form of NrdAB or an increased level of dNTPs contributed to the restoration of cell growth in the *hda* mutant. This is the first time an *nrdA* catalytic site mutant has been used to suggest that an elevated dNTP level is important for the rescue of an overinitiating mutant.

Cellular dNTP levels are elevated in cells bearing the *nrdAB* plasmid. We assessed cellular levels of dNTPs using two different methods (Fig. 5). First, we used a method in which DNA polymerase activity is assessed in vitro using a cell extract as the only source of dCTP (63). Cells were grown at 42°C and incubated at 25°C for 8 h, followed by preparation of dNTP extracts and DNA replication assay. The dCTP levels in the cell extracts were deduced using a standard dCTP solution (Fig. 5A). The dCTP level in the *hda-185* cells was elevated about twofold, depending on pBR322 bearing *nrdAB*. In the wild-type cells, the dCTP level was elevated about 1.5-fold, depending on the same plasmid. These results are consistent with a previous study that used pBR322 bearing *nrdAB* (63). In the presence of pBR322 excluding *nrdAB*, the dCTP level in the *hda-185* cells was significantly lower than that in the wild-type cells. This might be caused by the elevated ATP-DnaA level and transcriptional repression of the chromosomal *nrdAB* genes in the *hda-185* cells. ATP-DnaA represses the *nrdAB* transcription more effectively than ADP-DnaA did (16).

Second, we assessed cellular dATP levels using two-dimensional thin-layer chromatography. Cells were grown at 25°C in a phosphate-limited medium in the presence of $^{32}PO_4$, the

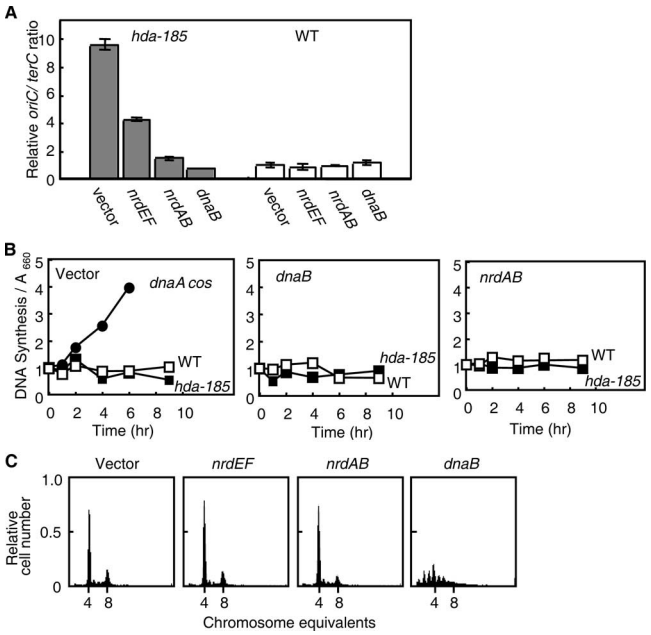

FIG. 6. Multiple copies of *dnaB*, *nrdAB*, or *nrdEF* repress overinitiation in the *hda-185* strain. (A) *oriC*/*terC* ratio. YH014 (wild-type *hda* [WT]) or YH013 (*hda-185*) cells carrying the indicated plasmid (vector, pBR322; *nrdEF*, pTKM221; *nrdAB*, pTKM226; *dnaB*, pTKM103) were grown at 42°C in LB medium containing ampicillin (50 μg/ml) until the optical density (A_{660}) reached 0.4, then diluted 400-fold, and incubated at 25°C for 8 h. The *oriC*/*terC* ratio of each sample was determined using quantitative PCR as described in Materials and Methods. Duplicate samples were used for this assay, and standard deviations (error bars) are shown. (B) Chromosomal DNA synthesis. YH014 (WT) and YH013 (*hda-185*) cells carrying the plasmid were grown at 42°C and further incubated at 25°C for the indicated times. Plasmids used are described above. NA001 (*dnaA cos*) cells were grown at 42°C and further incubated at 30°C for the indicated times, before being used as a positive control. Chromosomal DNA synthesis was measured as described in the legend to Fig. 2B. The incorporated ^{3}H counts at time zero in the deduced samples (0.5 ml) were 5.2 to 7.6 $\times$ 10^3, 6.5 to 9.3 $\times$ 10^3, and 3.4 $\times$ 10^3 cpm for YH014, YH013, and NA001, respectively. (C) Flow cytometry analysis. YH014 cells carrying the plasmid were exponentially grown at 25°C in LB medium containing ampicillin (50 μg/ml) and further incubated for 4 h in the presence of rifampin and cephalexin, followed by flow cytometry analysis. The plasmids that were used are described in the legend for panel A.

total cell volume was normalized, and the cell extracts were analyzed. The dATP level in the wild-type cells was elevated considerably, depending on pBR322 bearing *nrdAB* (Fig. 5B), consistent with a previous report (63). In the presence of the same plasmid, the dATP level in the *hda-185* cells was comparable to that in the wild-type cells (Fig. 5B), which is consistent with the dCTP level data (Fig. 5A). The levels of ATP and GTP were not significantly changed, which supports the specific effect of *nrdAB*. The *hda-185* cells bearing only vector pBR322 did not grow in a phosphate-limited medium.

Oversupply of DnaB or RNRs suppresses overinitiation in the *hda-185* mutant. We then asked whether the oversupply of DnaB or RNR inhibits overinitiation by assessing the *ori*/*ter* ratio using quantitative real-time PCR (Fig. 6A). Introduction of pBR322 derivatives carrying *dnaB* or *nrdAB* into *hda-185* cells repressed the *ori*/*ter* ratio to levels that were essentially the same as those of wild-type cells. Similar results were also obtained for the pBR322 derivative carrying *nrdEF*, but in this case, moderate inhibition was observed.

The function of these suppressors to repress the *ori*/*ter* ratio in the *hda-185* cells can be explained by either the repression of overinitiation or the release of the fork progression block. To distinguish these possibilities, we investigated DNA synthesis and found that an increase in overall chromosomal replication was not observed at 25°C in the *hda-185* strain harboring the *dnaB* plasmid or the *nrdAB* plasmid or in the strain harboring a control vector (Fig. 6B). These results indicate that the suppressor genes repress overinitiation in the *hda-185* strain. These results are the first to demonstrate that an oversupply of NrdAB, NrdEF, or DnaB inhibits overinitiation of chromosomal replication.

We further assessed using flow cytometry replication modes in the suppressed cells. If the oversupply of DnaB or NrdAB enhanced the replication fork movement without repressing overinitiation, the suppressed *hda-185* cells should have an increased ratio of DNA/mass at 25°C compared to the ratio of the wild-type cells. However, the DNA/mass ratio of the suppressed cells at 25°C was similar to that of the wild-type cells (Table 7). These results agree with the overall DNA synthesis/total cell volume data (Fig. 6B) and the idea that overinitiation is repressed in the suppressed cells. We do not exclude the possibility that the oversupply of DnaB or NrdAB enhanced the replication fork movement at 25°C in *hda-185* cells.

Abnormal interactions between DnaA and DnaB might affect the repressor function of DnaA (42, 57). Indeed, *dnaA* transcription is negatively autoregulated by DnaA protein. We examined the *dnaA* mRNA level in *hda-185* cells harboring the *dnaB* plasmid. Even at 25°C, the level of *dnaA* mRNA in these cells was comparable to the level in wild-type *hda* cells harboring the *dnaB* plasmid (Fig. 3C). Similar results were also obtained using the quantitative S1 nuclease assay (Fig. 3D).

Initiation modes in the wild-type cells bearing multiple copies of *nrdAB* or *dnaB*. We further examined the effects of multiple copies of the *dnaB* and *nrd* genes on the initiation of replication in the wild-type *hda* strain. Growing cells were incubated for 4 h in the presence of rifampin and cephalexin, followed by analysis by flow cytometry (Fig. 6C). The wild-type strains harboring pBR322, pBR322-*nrdAB*, or pBR322-*nrdEF*

TABLE 7. Relative cell mass and DNA content in the suppressed cells[a]

Strain/plasmid	Relative cell mass	Relative DNA content per cell	Relative DNA per mass
YH014 (*hda*$^+$)/pBR322 (vector)	1.0	1.0	1.0
YH014/pTKM221 (*nrdEF*)	1.0	1.1	1.1
YH014/pTKM226 (*nrdAB*)	1.0	1.1	1.1
YH014/pTKM103 (*dnaB*)	1.2	1.0	0.8
YH013 (*hda-185*)/pTKM221	3.0	2.2	0.7
YH013/pTKM226	1.5	1.6	1.1
YH013/pTKM103	1.3	1.1	0.8

[a] Cells of the indicated strains were grown at 25°C in LB medium containing ampicillin (50 μg/ml) until an optical density (A_{660}) reached 0.2. Cell mass and DNA content per cell were determined using flow cytometry as described in Materials and Methods. The values obtained for strain YH014 bearing pBR322 are defined as 1, and relative values are shown compared to this value. Plasmids were pBR322 (vector), pTKM221 (*nrdEF*), pTKM226 (*nrdAB*), and pTKM103 (*dnaB*).

predominantly contained four or eight chromosomes in a single cell at 25°C. In contrast, the wild-type strain harboring pBR322-*dnaB* showed a decreased DNA content and contained peaks of three, five, or six chromosomes, indicating that excessive DnaB inhibits initiation and thus causes asynchronous initiations. Excessive interaction between DnaA and DnaB might inhibit the actions of DnaA in the initiation processes, which might result in repression of overinitiation (Fig. 6A and B).

Effect of the LexA regulon on the *hda-185* strain. Microscopic analysis of the *hda-185* cells revealed that after incubation at nonpermissive temperatures for 8 h, this mutant forms filamentous cells (Fig. 7A). At 25°C, filamentation of the *hda-185* cells could be observed when the cells were incubated for 4 h or longer (data not shown). Flow cytometry suggested that after incubation at 25°C for 8 h, the *hda-185* cells were approximately seven times longer than the wild cells (Fig. 7B).

Cell division in the *dnaA cos* mutant is inhibited at 30°C in an *sfiA*-independent manner (28). In order to determine whether the SOS pathway affects cell division in the *hda-185* strain, we introduced an *sfiA* deletion or a *lexA3* mutation. The *lexA3* mutation renders LexA resistant to RecA*-induced cleavage, and thus, the SOS regulon is constitutively repressed (43). When we examined colony formation at 25°C, the Δ*sfiA hda-185* mutant exhibited a more severe inhibition of cell growth than the wild-type *sfiA hda-185* mutant did (Fig. 7C). The *lexA3* mutation also enhanced growth inhibition in the *hda-185* mutant at 25°C (Fig. 7C). It is conceivable that by the fork progression block, SOS genes, such as *sfiA*, are induced at low levels in the *hda-185* mutant at 25°C, enhancing survival of the mutant cells (see Discussion).

The Δ*sfiA hda-185* mutant formed filamentous cells at 25°C, and its average cell mass was similar to that of the wild-type *sfiA hda-185* strain (Fig. 7A and B). A similar result was obtained using the *lexA3 hda-185* strain (Fig. 7A and B). Thus, these results indicate that an *sfiA*-independent inhibition of cell division occurs due to defects in *hda* function.

The SlmA protein blocks FtsZ ring formation in the vicinity of nucleoids, which subsequently prevents untimely cell division (4). This form of regulation is termed nucleoid occlusion (4). We did not observe any significant effects of *slmA* deletion on cell size or cold sensitivity in the *hda-185* mutant at 25°C (Fig. 7A to C). These results suggest that the pathway blocking cell division in the *hda-185* mutant is independent of the nucleoid occlusion system.

DISCUSSION

In this study, we isolated a novel cold-sensitive *hda* allele, *hda-185*, and analyzed modes of chromosomal replication, *dnaA* expression, and cell division in the *hda-185* mutant. Notably, we found that multicopy supply of *dnaB*, *nrdAB*, or *nrdEF* inhibits overinitiation. Previously, oversupply of NrdAB or DnaB has been shown to repress the growth defect of *hda*-deleted cells or that of *dnaA219* overinitiation mutant cells, respectively (16, 54); however, it has not been demonstrated whether overinitiation of chromosomal replication is inhibited in the suppressed cells. Furthermore, we demonstrated that multiple copies of *nrdAB* increase the cellular dATP and dCTP levels in *hda-185* cells and a critical residue in

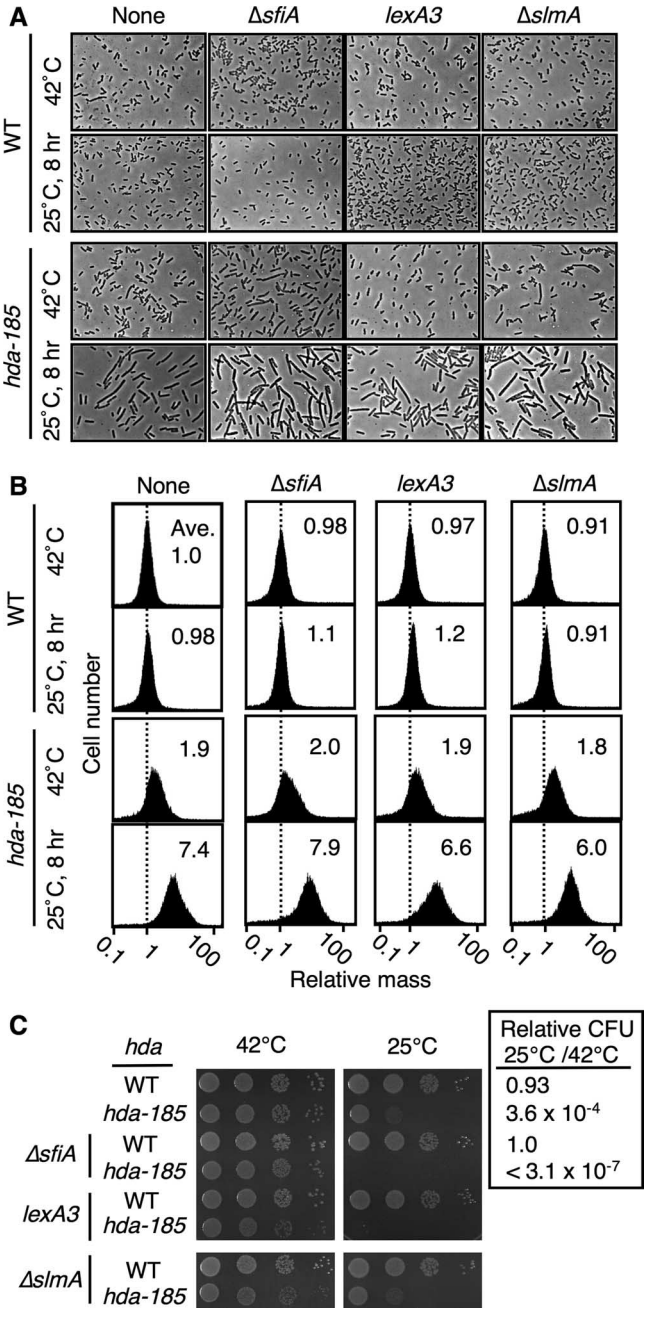

FIG. 7. Inhibition of cell division at a restrictive temperature. (A) Cell morphology. Cells were grown in LB medium at 42°C until the optimal density (A_{660}) reached 0.4, before the cells were diluted and incubated at 25°C for 8 h. These cells were fixed in methanol and observed by phase-contrast microscopy. The strains used and their relevant genotypes were as follows: YH014, wild-type *hda* (WT); YH013, *hda-185*; MZ002, Δ*sfiA*::*cat*; MZ001, *hda-185* Δ*sfiA*::*cat*; YH101, *lexA3*; YH102, *hda-185 lexA3*; YH103, Δ*slmA*; and YH104, *hda-185* Δ*slmA*. (B) Cell mass of the *hda-185* strain and its derivatives. Cells were incubated as described above and analyzed by flow cytometry. The relative size of the cells at the indicated temperatures was determined by measuring forward light scatter and is shown by the horizontal axis in logarithmic scale (Relative mass). The strains that were used are as described above for panel A. (C) Viability of the *hda-185* strain and its derivatives. Cells were grown overnight at 42°C, serially diluted, spotted on LB plates, and incubated at 42°C for 12 h or at 25°C for 27 h. In parallel, the CFU was determined by plating the overnight cultures on LB plates and incubating at 25°C and 42°C. The strains that were used are as described above for panel A.

the NrdA catalytic center is required for the *hda-185* suppression. These findings suggest a possible link between the replicational initiation system and the dNTP pool level. In addition, we found that cell division is inhibited at 25°C in *hda-185* cells in an *sfiA*-independent manner. This *sfiA*-independent system is unique in operating independently of the LexA regulon. An unrevealed regulatory mechanism would inhibit cell division upon overinitiation of chromosomal replication in the *hda* mutant.

The increased dNTP level or an active form of NrdAB might be related to the repression of overinitiation in the *hda-185* cells (Fig. 5 and 6; Table 6). The repression would be specific to extra initiation events because initiation in the wild-type cells was not inhibited by multiple copies of *nrdAB* (Fig. 6C). A possible linkage mechanism between the dNTP levels and the initiation regulatory systems might be that the elevated dNTP level results in functional inhibition of a protein involved in replication initiation. For example, in *Saccharomyces cerevisiae*, it has been reported that constitutively elevated dNTP levels result in inhibition of the entry into S phase in a manner concomitant with reduced chromatin loading of Cdc45, a component of replication initiation (8). Alternatively, the dNTP levels might affect the expression of DNA replication-related genes. For example, NrdR is a transcriptional repressor for *nrdAB* and *nrdEF* (61), and the NrdR homolog in *Streptomyces coelicolor* shows dATP/ATP-dependent binding to a specific DNA in vitro (18). The NrdR-binding consensus (NrdR box) is seen in the promoter region of *dnaA* in *Shewanella* spp. and in *Myxococcus xanthus* and *topA* in *Pseudomonas* spp. (53).

The *hda-185* mutant causes *sfiA*-independent inhibition of cell division at nonpermissive temperatures (Fig. 7). Previously, mitomycin has been shown to induce an *sfi*-independent division inhibition in a manner depending on a gene included in the LexA regulon (20). The filamentation of *hda-185* mutant cells was independent of the LexA regulon, indicating that a division inhibition pathway in this mutant is distinct from the previously reported *sfi*-independent pathway. Nalidixic acid or thymine starvation, which causes inhibition of the replication fork progression, is reported to lead to a reduction in the transcription of the FtsZ operon (37). Although the mechanism causing this reduction remains to be elucidated, it could be related to our observations in this study. At present, only limited investigations have been performed for the mechanisms regulating cell division in cells causing overinitiation of chromosomal replication (28).

Also, we noticed an unexpected role for SfiA in the survival of *hda-185* cells at 25°C: the colony formation defect in the *hda-185* mutant at 25°C was enhanced by *sfiA* disruption (Fig. 7C). The replication fork block in the *hda-185* strain could activate the SfiA division inhibition system via the SOS response. SfiA inhibition of FtsZ ring formation is reported to be reversible (39). We speculate that the SfiA system keeps cells viable, resulting in an enhanced occurrence of suppressor mutations. In the absence of *sfiA*, an *sfiA*-independent system would be complementarily induced in the *hda-185* cells. It is conceivable that this system inhibits the cell division process at a point later than the SfiA-inhibiting point and causes adverse effects on the viability of the cells.

The cellular levels of *dnaA* mRNA and DnaA in the *hda-185* cells at 25°C were similar to those in the wild-type cells (Fig. 2D and 3). Also, a moderate increase in the ATP-DnaA level was seen in an *hda-185*-dependent manner (Fig. 4). Thus, factors other than ATP-DnaA might sustain the *dnaA* transcriptional regulation more effectively in vivo, whereas in vitro, ATP-DnaA represses the *dnaA* promoter activity more tightly than ADP-DnaA does (57). Indeed, in vivo experiments using replication cycle-synchronized cells demonstrate that the *dnaA* promoter activity is tightly repressed in the postinitiation period in which the ATP-DnaA level is decreased and the ADP-DnaA level is elevated by RIDA (6, 36). A recent report has indicated that the DnaA protein level is reduced in *hda*-deficient cells to ~50 to 60% of the wild-type level (52); however, the *hda*-deficient cells used in that study carry the *hsm-1* suppressor mutation (*hda* suppressor mutation). The gene bearing the *hsm-1* mutation has not been identified. The possibility that the wild-type *hsm* gene product directly or indirectly regulates the *dnaA* transcription and that the *hsm-1* mutation reduces the *dnaA* transcription level in the absence of Hda, resulting in suppression of the growth defect in *hda*-deficient cells, might be important.

The mutation site (K185C) within the *hda-185* allele is located in the AAA+ domain that Hda and DnaA share (29). The basic moiety at this position is highly conserved among the orthologs of DnaA and Hda in many bacterial species. The crystal structure of the *Aquifex aeolicus* DnaA AAA+ domain shows that the residue (Arg-246) corresponding to the Hda Lys-185 residue resides on an α-helix of the C-terminal subdomain (domain IIIb) and its basic side chain is located inside the protein structure (14, 15). The substitution of K185C might destabilize the whole conformation of the C-terminal subdomain and thus render the Hda function temperature dependent.

ACKNOWLEDGMENTS

We are grateful to Tomomi Wakatsuki for strain construction, Takuma Ishida for plasmid construction, and Jun-ichi Kato, Takashi Hishida, and Hironori Niki for strains.

This study was mainly supported by grants-in-aid from the Ministry of Education, Culture, Sports, Science and Technology of Japan.

REFERENCES

1. **Abe, Y., T. Jo, Y. Matsuda, C. Matsunaga, T. Katayama, and T. Ueda.** 2007. Structure and function of DnaA N-terminal domains: specific sites and mechanisms in inter-DnaA interaction and in DnaB helicase loading on *oriC*. J. Biol. Chem. **282:**17816–17827.
2. **Aberg, A., S. Hahne, M. Karlsson, A. Larsson, M. Ormo, A. Ahgren, and B. M. Sjöberg.** 1989. Evidence for two different classes of redox-active cysteines in ribonucleotide reductase of *Escherichia coli*. J. Biol. Chem. **264:**12249–12252.
3. **Baba, T., T. Ara, M. Hasegawa, Y. Takai, Y. Okumura, M. Baba, K. A. Datsenko, M. Tomita, B. L. Wanner, and H. Mori.** 2006. Construction of *Escherichia coli* K-12 in-frame, single-gene knockout mutants: the Keio collection. Mol. Syst. Biol. **2:**2006.0008.
4. **Bernhardt, T. G., and P. A. de Boer.** 2005. SlmA, a nucleoid-associated, FtsZ binding protein required for blocking septal ring assembly over chromosomes in *E. coli*. Mol. Cell **18:**555–564.
5. **Bochner, B. R., and B. N. Ames.** 1982. Complete analysis of cellular nucleotides by two-dimensional thin layer chromatography. J. Biol. Chem. **257:**9759–9769.
6. **Bogan, J. A., and C. E. Helmstetter.** 1997. DNA sequestration and transcription in the *oriC* region of *Escherichia coli*. Mol. Microbiol. **26:**889–896.
7. **Camara, J. E., A. M. Breier, T. Brendler, S. Austin, N. R. Cozzarelli, and E. Crooke.** 2005. Hda inactivation of DnaA is the predominant mechanism preventing hyperinitiation of *Escherichia coli* DNA replication. EMBO Rep. **6:**736–741.
8. **Chabes, A., and B. Stillman.** 2007. Constitutively high dNTP concentration inhibits cell cycle progression and the DNA damage checkpoint in yeast *Saccharomyces cerevisiae*. Proc. Natl. Acad. Sci. USA **104:**1183–1188.

9. **Courcelle, J., and P. C. Hanawalt.** 2003. RecA-dependent recovery of arrested DNA replication forks. Annu. Rev. Genet. **37:**611–646.
10. **Dalrymple, B. P., K. Kongsuwan, G. Wijffels, N. E. Dixon, and P. A. Jennings.** 2001. A universal protein-protein interaction motif in the eubacterial DNA replication and repair systems. Proc. Natl. Acad. Sci. USA **98:**11627–11632.
11. **d'Ari, R.** 1985. The SOS system. Biochimie **67:**343–347.
12. **Datsenko, K. A., and B. L. Wanner.** 2000. One-step inactivation of chromosomal genes in *Escherichia coli* K-12 using PCR products. Proc. Natl. Acad. Sci. USA **97:**6640–6645.
13. **Ekberg, M., P. Birgander, and B. M. Sjöberg.** 2003. In vivo assay for low-activity mutant forms of *Escherichia coli* ribonucleotide reductase. J. Bacteriol. **185:**1167–1173.
14. **Erzberger, J. P., M. L. Mott, and J. M. Berger.** 2006. Structural basis for ATP-dependent DnaA assembly and replication-origin remodeling. Nat. Struct. Mol. Biol. **13:**676–683.
15. **Erzberger, J. P., M. M. Pirruccello, and J. M. Berger.** 2002. The structure of bacterial DnaA: implications for general mechanisms underlying DNA replication initiation. EMBO J. **21:**4763–4773.
16. **Gon, S., J. E. Camara, H. K. Klungsoyr, E. Crooke, K. Skarstad, and J. Beckwith.** 2006. A novel regulatory mechanism couples deoxyribonucleotide synthesis and DNA replication in *Escherichia coli*. EMBO J. **25:** 1137–1147.
17. **Grigorian, A. V., R. B. Lustig, E. C. Guzman, J. M. Mahaffy, and J. W. Zyskind.** 2003. *Escherichia coli* cells with increased levels of DnaA and deficient in recombinational repair have decreased viability. J. Bacteriol. **185:**630–644.
18. **Grinberg, I., T. Shteinberg, B. Gorovitz, Y. Aharonowitz, G. Cohen, and I. Borovok.** 2006. The *Streptomyces* NrdR transcriptional regulator is a Zn ribbon/ATP cone protein that binds to the promoter regions of class Ia and class II ribonucleotide reductase operons. J. Bacteriol. **188:**7635–7644.
19. **Guo, L., T. Katayama, Y. Seyama, K. Sekimizu, and T. Miki.** 1999. Isolation and characterization of novel cold-sensitive *dnaA* mutants of *Escherichia coli*. FEMS Microbiol. Lett. **176:**357–366.
20. **Hill, T. M., B. Sharma, M. Valjavec-Gratian, and J. Smith.** 1997. *sfi*-independent filamentation in *Escherichia coli* is *lexA* dependent and requires DNA damage for induction. J. Bacteriol. **179:**1931–1939.
21. **Ishida, T., N. Akimitsu, T. Kashioka, M. Hatano, T. Kubota, Y. Ogata, K. Sekimizu, and T. Katayama.** 2004. DiaA, a novel DnaA-binding protein, ensures the timely initiation of *Escherichia coli* chromosome replication. J. Biol. Chem. **279:**45546–45555.
22. **Kaguni, J. M.** 2006. DnaA: controlling the initiation of bacterial DNA replication and more. Annu. Rev. Microbiol. **60:**351–375.
23. **Katayama, T.** 1994. The mutant DnaAcos protein which overinitiates replication of the *Escherichia coli* chromosome is inert to negative regulation for initiation. J. Biol. Chem. **269:**22075–22079.
24. **Katayama, T., N. Akimitsu, T. Mizushima, T. Miki, and K. Sekimizu.** 1997. Overinitiation of chromosome replication in the *Escherichia coli dnaAcos* mutant depends on activation of *oriC* function by the *dam* gene product. Mol. Microbiol. **25:**661–670.
25. **Katayama, T., and E. Crooke.** 1995. DnaA protein is sensitive to a soluble factor and is specifically inactivated for initiation of *in vitro* replication of the *Escherichia coli* minichromosome. J. Biol. Chem. **270:**9265–9271.
26. **Katayama, T., and A. Kornberg.** 1994. Hyperactive initiation of chromosomal replication *in vivo* and *in vitro* by a mutant initiator protein, DnaAcos, of *Escherichia coli*. J. Biol. Chem. **269:**12698–12703.
27. **Katayama, T., T. Kubota, K. Kurokawa, E. Crooke, and K. Sekimizu.** 1998. The initiator function of DnaA protein is negatively regulated by the sliding clamp of the *E. coli* chromosomal replicase. Cell **94:**61–71.
28. **Katayama, T., M. Takata, and K. Sekimizu.** 1997. CedA is a novel *Escherichia coli* protein that activates the cell division inhibited by chromosomal DNA over-replication. Mol. Microbiol. **26:**687–697.
29. **Kato, J., and T. Katayama.** 2001. Hda, a novel DnaA-related protein, regulates the replication cycle in *Escherichia coli*. EMBO J. **20:**4253–4262.
30. **Kawakami, H., T. Iwura, M. Takata, K. Sekimizu, S. Hiraga, and T. Katayama.** 2001. Arrest of cell division and nucleoid partition by genetic alterations in the sliding clamp of the replicase and in DnaA. Mol. Genet. Genomics **266:**167–179.
31. **Kawakami, H., S. Ozaki, S. Suzuki, K. Nakamura, T. Senriuchi, M. Su'etsugu, K. Fujimitsu, and T. Katayama.** 2006. The exceptionally tight affinity of DnaA for ATP/ADP requires a unique aspartic acid residue in the AAA+ sensor 1 motif. Mol. Microbiol. **62:**1310–1324.
32. **Kellenberger-Gujer, G., A. J. Podhajska, and L. Caro.** 1978. A cold sensitive dnaA mutant of *E. coli* which overinitiates chromosome replication at low temperature. Mol. Gen. Genet. **162:**9–16.
33. **Keyamura, K., N. Fujikawa, T. Ishida, S. Ozaki, M. Su'etsugu, K. Fujimitsu, W. Kagawa, S. Yokoyama, H. Kurumizaka, and T. Katayama.** 2007. The interaction of DiaA and DnaA regulates the replication cycle in *E. coli* by directly promoting ATP DnaA-specific initiation complexes. Genes Dev. **21:**2083–2099.
34. **Kitagawa, R., T. Ozaki, S. Moriya, and T. Ogawa.** 1998. Negative control of replication initiation by a novel chromosomal locus exhibiting exceptional affinity for *Escherichia coli* DnaA protein. Genes Dev. **12:**3032–3043.
35. **Kogoma, T.** 1997. Stable DNA replication: interplay between DNA replication, homologous recombination, and transcription. Microbiol. Mol. Biol. Rev. **61:**212–238.
36. **Kurokawa, K., S. Nishida, A. Emoto, K. Sekimizu, and T. Katayama.** 1999. Replication cycle-coordinated change of the adenine nucleotide-bound forms of DnaA protein in *Escherichia coli*. EMBO J. **18:**6642–6652.
37. **Liu, G., K. Begg, A. Geddes, and W. D. Donachie.** 2001. Transcription of essential cell division genes is linked to chromosome replication in *Escherichia coli*. Mol. Microbiol. **40:**909–916.
38. **Lu, M., J. L. Campbell, E. Boye, and N. Kleckner.** 1994. SeqA: a negative modulator of replication initiation in *E. coli*. Cell **77:**413–426.
39. **Maguin, E., J. Lutkenhaus, and R. D'Ari.** 1986. Reversibility of SOS-associated division inhibition in *Escherichia coli*. J. Bacteriol. **166:**733–738.
40. **Marszalek, J., W. Zhang, T. R. Hupp, C. Margulies, K. M. Carr, S. Cherry, and J. M. Kaguni.** 1996. Domains of DnaA protein involved in interaction with DnaB protein, and in unwinding the *Escherichia coli* chromosomal origin. J. Biol. Chem. **271:**18535–18542.
41. **Messer, W.** 2002. The bacterial replication initiator DnaA. DnaA and *oriC*, the bacterial mode to initiate DNA replication. FEMS Microbiol. Rev. **26:**355–374.
42. **Messer, W., and C. Weigel.** 1997. DnaA initiator—also a transcription factor. Mol. Microbiol. **24:**1–6.
43. **Mount, D. W., K. B. Low, and S. J. Edmiston.** 1972. Dominant mutations (*lex*) in *Escherichia coli* K-12 which affect radiation sensitivity and frequency of ultraviolet light-induced mutations. J. Bacteriol. **112:**886–893.
44. **Mukherjee, A., C. Cao, and J. Lutkenhaus.** 1998. Inhibition of FtsZ polymerization by SulA, an inhibitor of septation in *Escherichia coli*. Proc. Natl. Acad. Sci. USA **95:**2885–2890.
45. **Neuwald, A. F., L. Aravind, J. L. Spouge, and E. V. Koonin.** 1999. AAA+: a class of chaperone-like ATPases associated with the assembly, operation, and disassembly of protein complexes. Genome Res. **9:**27–43.
46. **Nievera, C., J. J. Torgue, J. E. Grimwade, and A. C. Leonard.** 2006. SeqA blocking of DnaA-*oriC* interactions ensures staged assembly of the *E. coli* pre-RC. Mol. Cell **24:**581–592.
47. **Nishida, S., K. Fujimitsu, K. Sekimizu, T. Ohmura, T. Ueda, and T. Katayama.** 2002. A nucleotide switch in the *Escherichia coli* DnaA protein initiates chromosomal replication: evidence from a mutant DnaA protein defective in regulatory ATP hydrolysis *in vitro* and *in vivo*. J. Biol. Chem. **277:**14986–14995.
48. **Nordlund, P., and P. Reichard.** 2006. Ribonucleotide reductases. Annu. Rev. Biochem. **75:**681–706.
49. **O'Donnell, M.** 2006. Replisome architecture and dynamics in *Escherichia coli*. J. Biol. Chem. **281:**10653–10656.
50. **Ogawa, T., and T. Okazaki.** 1994. Cell cycle-dependent transcription from the *gid* and *mioC* promoters of *Escherichia coli*. J. Bacteriol. **176:**1609–1615.
51. **Ote, T., M. Hashimoto, Y. Ikeuchi, M. Su'etsugu, T. Suzuki, T. Katayama, and J. Kato.** 2006. Involvement of the *Escherichia coli* folate-binding protein YgfZ in RNA modification and regulation of chromosomal replication initiation. Mol. Microbiol. **59:**265–275.
52. **Riber, L., J. A. Olsson, R. B. Jensen, O. Skovgaard, S. Dasgupta, M. G. Marinus, and A. Løbner-Olesen.** 2006. Hda-mediated inactivation of the DnaA protein and *dnaA* gene autoregulation act in concert to ensure homeostatic maintenance of the *Escherichia coli* chromosome. Genes Dev. **20:**2121–2134.
53. **Rodionov, D. A., and M. S. Gelfand.** 2005. Identification of a bacterial regulatory system for ribonucleotide reductases by phylogenetic profiling. Trends Genet. **21:**385–389.
54. **Seitz, H., C. Weigel, and W. Messer.** 2000. The interaction domains of the DnaA and DnaB replication proteins of *Escherichia coli*. Mol. Microbiol. **37:**1270–1279.
55. **Shibata, T., T. Hishida, Y. Kubota, Y. W. Han, H. Iwasaki, and H. Shinagawa.** 2005. Functional overlap between RecA and MgsA (RarA) in the rescue of stalled replication forks in *Escherichia coli*. Genes Cells **10:**181–191.
56. **Slater, S., S. Wold, M. Lu, E. Boye, K. Skarstad, and N. Kleckner.** 1995. *E. coli* SeqA protein binds *oriC* in two different methyl-modulated reactions appropriate to its roles in DNA replication initiation and origin sequestration. Cell **82:**927–936.
57. **Speck, C., C. Weigel, and W. Messer.** 1999. ATP- and ADP-DnaA protein, a molecular switch in gene regulation. EMBO J. **18:**6169–6176.
58. **Su'etsugu, M., A. Emoto, K. Fujimitsu, K. Keyamura, and T. Katayama.** 2003. Transcriptional control for initiation of chromosomal replication in *Escherichia coli*: fluctuation of the level of origin transcription ensures timely initiation. Genes Cells **8:**731–745.
59. **Su'etsugu, M., T. Shimuta, T. Ishida, H. Kawakami, and T. Katayama.** 2005. Protein associations in DnaA-ATP hydrolysis mediated by the Hda-replicase clamp complex. J. Biol. Chem. **280:**6528–6536.
60. **Theisen, P. W., J. E. Grimwade, A. C. Leonard, J. A. Bogan, and C. E. Helmstetter.** 1993. Correlation of gene transcription with the time of initia-

tion of chromosome replication in *Escherichia coli*. Mol. Microbiol. **10:**575–584.
61. **Torrents, E., I. Grinberg, B. Gorovitz-Harris, H. Lundstrom, I. Borovok, Y. Aharonowitz, B. M. Sjöberg, and G. Cohen.** 2007. NrdR controls differential expression of the *Escherichia coli* ribonucleotide reductase genes. J. Bacteriol. **189:**5012–5021.
62. **Walker, G.** 1996. The SOS response of *Escherichia coli*, p. 1579–1601. *In* F. C. Neidhardt, R. Curtiss III, J. L. Ingraham, E. C. C. Lin, K. B. Low, B. Magasanik, W. S. Reznikoff, M. Riley, M. Schaechter, and H. E. Umbarger (ed.), *Escherichia coli* and *Salmonella*: cellular and molecular biology, 2nd ed. ASM Press, Washington, DC.
63. **Wheeler, L. J., I. Rajagopal, and C. K. Mathews.** 2005. Stimulation of mutagenesis by proportional deoxyribonucleoside triphosphate accumulation in *Escherichia coli*. DNA Repair (Amsterdam) **4:**1450–1456.